

Article

Extraction and Evaluation of Discriminative Indexes of the Wearing Condition for High-Precision Blood Pressure Pulse Wave Measurement

Yosuke Osawa * and Tetsuji Dohi *

Micro System Laboratory, Chuo University, 1-13-27, Kasuga, Bunkyo-ku, Tokyo 112-8551, Japan

* Correspondence: osawa@msl.mech.chuo-u.ac.jp (Y.O.); dohi@mech.chuo-u.ac.jp (T.D.)

Abstract: In this paper, we report a new discriminant index for evaluating the wearing condition of a blood pressure pulse wave measurement device with small variability. The prototype device consists of MEMS 3-axis force sensors, a 3-axis push-in adjustment mechanism, a fixed jig, and a signal processing board. The arterial tonometry method is used by this device to measure blood pressure pulse waves. However, to accurately measure the blood pressure pulse wave, the device must be appropriately worn. The evaluation of the wearing condition using the amplitude of the blood pressure pulse wave was complicated by the wearing process due to the large variability. Therefore, we propose the ratio of the blood pressure pulse wave component to the noise component as an index that can evaluate the wear condition of the device. The correlation coefficient between the discriminant index and the amplitude of the blood pressure pulse wave had a correlation coefficient of 0.879. Furthermore, the discriminant index reduced the coefficient of variation by 12.8%. Therefore, it was suggested that the discriminant index is an index that can evaluate the pressing amount, one of the wearing conditions of the blood pressure pulse wave measurement device with a small influence of variation.

Keywords: MEMS 3-axis sensor; arterial tonometry; blood pressure pulse wave



Citation: Osawa, Y.; Dohi, T. Extraction and Evaluation of Discriminative Indexes of the Wearing Condition for High-Precision Blood Pressure Pulse Wave Measurement. *Micromachines* **2022**, *13*, 679. <https://doi.org/10.3390/mi13050679>

Academic Editors: Takashi Tokumasu, Masahiro Motosuke, Takashi Abe and Tetsuo Kan

Received: 18 March 2022

Accepted: 22 April 2022

Published: 27 April 2022

Publisher's Note: MDPI stays neutral with regard to jurisdictional claims in published maps and institutional affiliations.



Copyright: © 2022 by the authors. Licensee MDPI, Basel, Switzerland. This article is an open access article distributed under the terms and conditions of the Creative Commons Attribution (CC BY) license (<https://creativecommons.org/licenses/by/4.0/>).

1. Introduction

Hypertension, in which high blood pressure continues, is said to accelerate arteriosclerosis and is said to be a cause of the increased risk of myocardial infarction and stroke [1]. In addition, blood pressure changes depending on one's state and environment such as during activity and rest and fluctuation during the day are also significant. Sudden changes in blood pressure, especially, may cause sudden changes in symptoms in cardiovascular disorders such as myocardial infarction and stroke [2]. As a result, it is important to detect these risks in advance by monitoring the rapid changes in blood pressure through continuous blood pressure measurement at each beat during daily life.

The oscillometric method is one of the most commonly used methods for measuring blood pressure in daily life. In this measurement method, the upper arm is pressurized by the air pressure of a cuff wrapped around the arm, and the systolic and diastolic pressures are measured by the pressure change during the decompression process [3]. Using this principle, there is Ambulatory Blood Pressure Monitoring (ABPM), which can measure blood pressure at a high frequency every 30 min. This device is not only unable to measure continuous blood pressure with each beat, but it has also been reported to cause acute neuralgia and sleep disturbance due to the high-pressure load [4,5], whereas arterial tonometry is one of the methods that can measure blood pressure continuously and with low load [6,7]. This method enables continuous and low-load blood pressure measurement as if palpated by a force sensor placed directly above the radial artery. On the other hand, to accurately measure blood pressure by this method, the device must be worn in the proper condition [8]. The following parameters are used to evaluate the wearing condition of

the device: the position of the sensor and the radial artery, the angle between the wrist and the sensor surface, and the amount of pressure on the sensor. Dueck and others showed good agreement between invasive and noninvasive radial artery blood pressures when the device was worn, such that the amplitude of the blood pressure pulse wave was maximized [9]. The amplitude of the blood pressure pulse wave increased with the sensor pressing force in this study, as shown in Figure 1, and the maximum amplitude value was used as an index to evaluate the wear condition of the arterial tonometry method. Kato and others developed a device with pressure sensor arrays that can be worn automatically with maximum amplitude using air pressure [10]. Furthermore, Canning and others developed a headphone-type sphygmomanometer and achieved blood pressure pulse wave measurement at the superficial temporal artery [11]. This device uses a stepping motor to automatically adjust the amount of pressure on the sensor so that measurements can be made according to the appropriate mounting condition. Although these devices can automatically adjust the wearing condition, creating wearable devices with motors and pneumatics is difficult because the devices are heavy and consume large amounts of electricity. In contrast, in our laboratory, we have been developing a wristwatch-type wearable device that is small, lightweight, and capable of continuously measuring blood pressure pulse waves [12–14]. A photograph of the latest prototype device is shown in Figure 2. While this device is small, lightweight, and can continuously measure blood pressure pulse waves, the wearing process is complicated and time-consuming for high-precision blood pressure measurement. Specifically, it is necessary to confirm that the amplitude of the blood pressure pulse wave is maximum at each of the following: the position of the sensor and radial artery, the angle between the wrist and sensor surface, and the amount of sensor pressure. Additionally, because the amplitude of the blood pressure pulse wave varies from measurement to measurement and has large variability, it is necessary to confirm it at each wear. Therefore, a discrimination index of the device's wearing state with small variability is required to make the evaluation of wear easier.

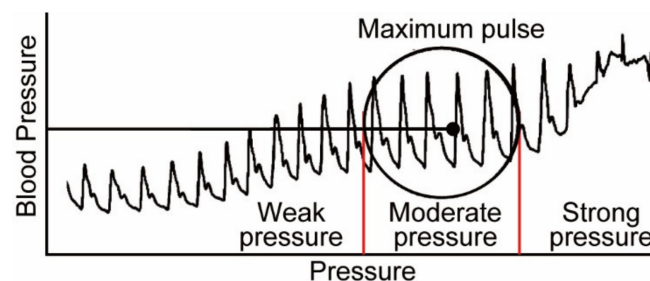


Figure 1. Changes in the amplitude of the blood pressure pulse wave when the wearing state is changed [9].



Figure 2. Wristwatch-type device being developed in our lab.

In this study, we developed a prototype device using the arterial tonometry method and measured blood pressure pulse waves while changing the wearing condition. Furthermore, the measured waveform is frequency analyzed to determine the discriminant index related to the wearing condition of the device. The purpose of this study is to confirm

whether the discriminant index can evaluate the wearing condition and if it is a small variation index.

2. Principle and Device

Figure 3 shows the principle of the tonometry method, which enables continuous blood pressure measurement for each beat [15]. The device is mounted so that the MEMS 3-axis force sensor is placed directly above the radial artery, as shown in Figure 3a. When the sensor is not pressed against the skin surface, the measured force differs from blood pressure because it includes the vertical component of the tension acting in the circumferential direction of the vessel wall. As shown in Figure 3b, we flatten the upper part of the vessel by pressing the force sensor vertically against the skin just above the vessel with moderate pressing force. The vertical component of the tension acting on the vessel wall is reduced to zero in this way, and the pressing force and blood pressure are balanced. Therefore, the force sensor can directly measure blood pressure. Unlike the oscillometric method, which is a common blood pressure measurement method, the arterial tonometry method can measure blood pressure in a minimally invasive and continuous manner, since the measurement method does not block blood flow.

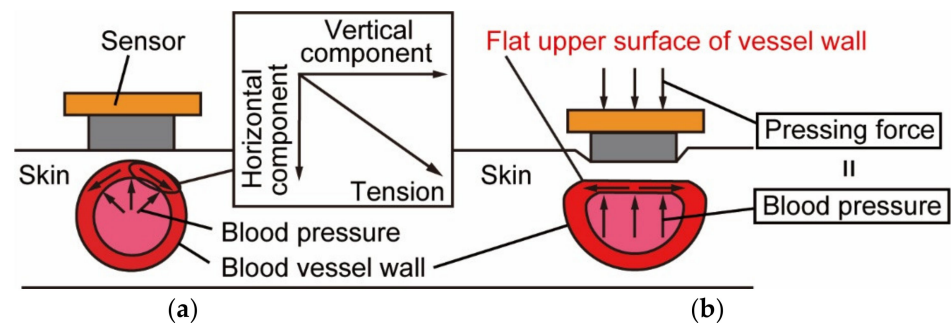


Figure 3. The principle of the arterial tonometry method: (a) Without pushing force; (b) With moderate pushing force.

The principle of the MEMS 3-axis force sensor used in this study is shown in Figure 4 [16]. The sensor shown in Figure 4a consists of three pairs of Si sidewall beams, one of which can measure vertical force and the other two can measure shear force. As an example, we will explain the principle of shear force measurement in this section. The beams formed in the sensor are arranged vertically, and the piezo-resistive layer is placed inside their sides. Since the MEMS 3-axis force sensor is embedded in the silicon rubber, the beam deforms in the direction of the force when the shear force is applied, as shown in Figure 4b. The resistance regions formed inside the two pairs expand and contract in the direction of deformation as the beams deform. The Wheatstone bridge circuit and the amplifier circuit detect the change in resistance due to the deformation of the beam, which is detected as a voltage change, and the shear force can be measured.

The appearance of the prototype device is shown in Figure 5. As shown in Figure 5a, the dimensions of the device are $95 \times 75 \times 45 \text{ mm}^3$. The prototype device consists of a MEMS 3-axis force sensor array, a fixed jig, a 3-axis push-in adjustment mechanism, and a signal processing board. The MEMS 3-axis force sensor array shown in Figure 5b was developed in collaboration with Shinano Kenshi Co., Ltd. (Ueda, Japan) and Touchence Co. (Tokyo, Japan), and consists of five force sensors arranged in a crisscross pattern. The sensor element is a sensor chip embedded with PDMS, and the distance between the sensors is 3.4 mm. Figure 5c shows a photograph of the sensor chip. The dimensions of the sensor chip are $2.0 \times 2.0 \times 0.3 \text{ mm}^3$, and the sampling frequency is 100 Hz. The fixed jig was fabricated using a 3D printer and can restrain the wrist. The 3-axis push-in adjustment mechanism can adjust the position and angle of the radial artery and sensor.

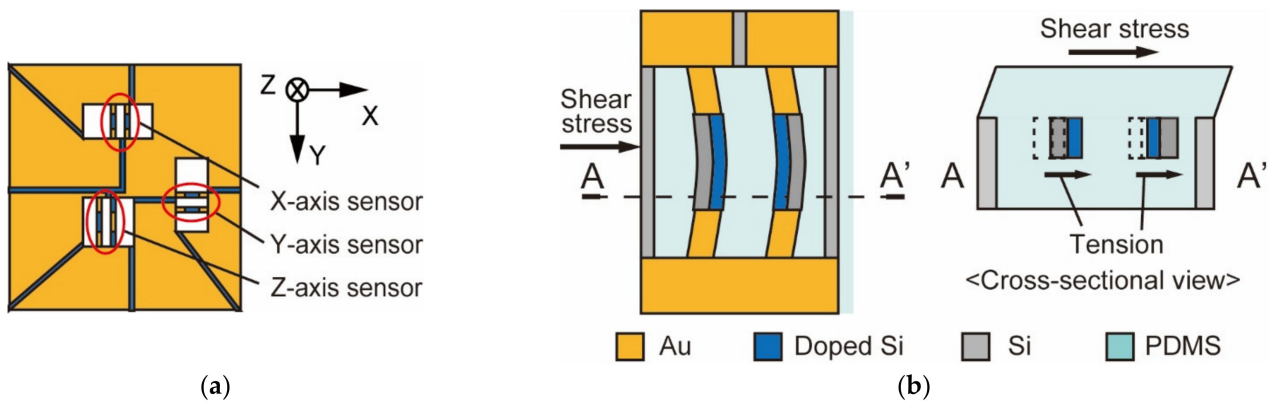


Figure 4. MEMS 3-axis force sensor: (a) Overview of the sensor; (b) The principle of the sensor.

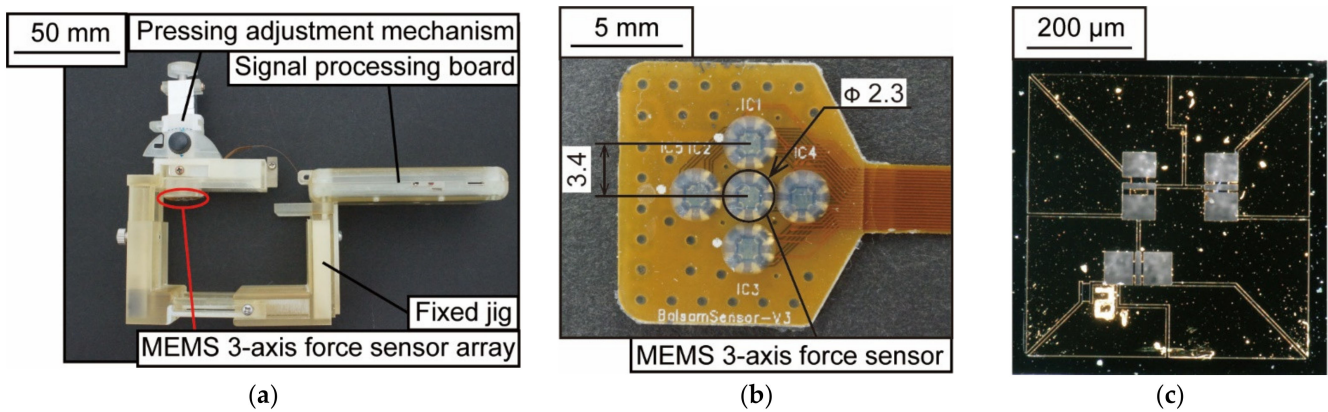


Figure 5. A photograph of the blood pressure pulse wave measurement device: (a) Wearable device; (b) MEMS 3-axis force sensor array; (c) Force sensor chip.

3. Experiments and Results

We experimented to measure blood pressure pulse waves in the resting sitting position to confirm that the prototype can measure blood pressure. Figure 6a shows a photograph of the device, which was worn on the left wrist during the experiment. A healthy 25-year-old male subject participated in the measurement. The measurement waveform is shown in Figure 6b. The vertical axis represents the measured force F [mN], and the horizontal axis represents the measurement time T [s]. Local maxima and local minima could be confirmed periodically from the measurement form, and a single beat of the blood pressure pulse wave was extracted. The results of the Fourier transform of the extracted waveforms are shown in Figure 6c. It can be seen that the spectral intensity of the blood pressure pulse wave is quite low at $f > 20$ Hz. It is also known that at $0 < f \leq 2$ Hz, the heart rate is greatly affected by the main elements of the heart rate [17]. Therefore, the cut-off frequency f_c is determined between $2 < f \leq 20$ Hz. Then, the value of the integral for $2 < f \leq f_c$ is defined as the low-frequency component (LF), and the value of the integral for $f > f_c$ is defined as the high-frequency component (HF). The ratio of LF to HF (LF/HF) is proposed as an index to discriminate the wearing condition of the device.

Next, to confirm that the proposed discriminant index LF/HF (f_c) is related to the device wearing state, blood pressure pulse wave measurement is conducted while varying the pressing amount of the sensor. The wearing condition of the device includes the pressing amount of the sensor, its position, and the sensor surface angle. In this experiment, the position of the sensor and the angle of the sensor surface were adjusted so that the amplitude of the pulse wave was always at its maximum. In this state, the pressing amount d [mm] shown in Figure 6a was increased by 1 mm every 20 s. The initial value of the pressing amount d was set at the position where the sensor made contact with the skin,

and the experiment was conducted until the amplitude of the blood pressure pulse wave attenuated and disappeared.

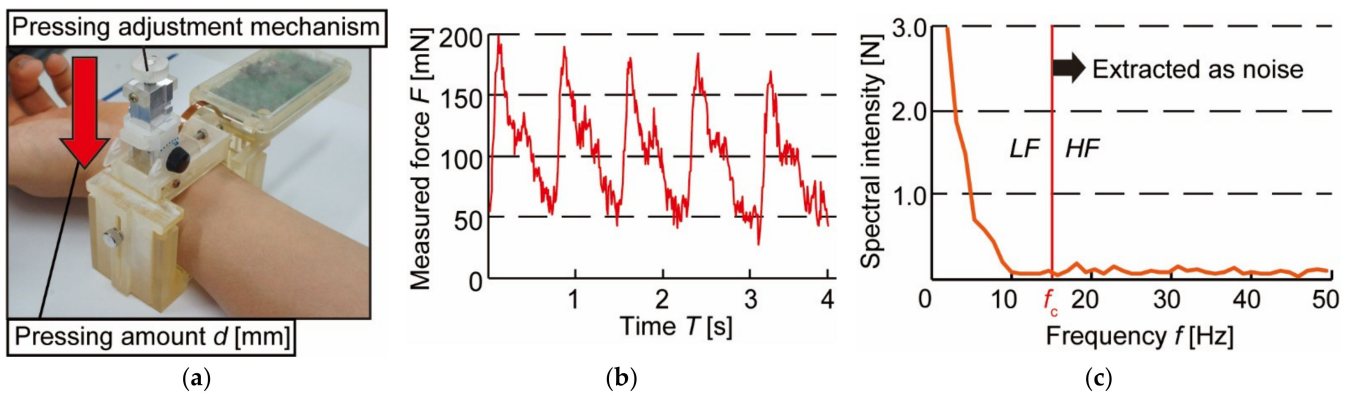


Figure 6. Experimental conditions and results of blood pressure pulse wave measurement: (a) Experimental setup; (b) Waveform of blood pressure pulse wave; (c) Fourier transformed blood pressure pulse wave.

The measurement waveform is shown in Figure 7a. The vertical axis represents the measured force F [N], and the horizontal axis represents the measurement time T [s]. In this experiment, the blood pressure pulse wave for each beat was extracted from the measured waveform and Fourier transformed as in the previous experiment. The discrimination indices LF/HF were calculated by varying the cut-off frequency f_c . We then confirmed the relationship between LF/HF , and the amplitude of the blood pressure pulse wave, A_P , which can evaluate the wearing state of the device. The correlation coefficients between LF/HF and A_P are shown in Figure 7b when f_c is varied. The correlation coefficient was maximum at $f_c = 7.3$ Hz and showed a very strong correlation of $R = 0.924$. This suggests that it is possible to discriminate against the wearing state of a device by LF/HF .

Finally, to confirm the variability of the discrimination index LF/HF , we conducted 20 repetition experiments of changing the wearing condition. When the cut-off frequency f_c is varied, the correlation coefficient between LF/HF and the amplitude of the blood pressure pulse wave A_P is shown in Figure 8a. The results of the 20 experiments also show that the correlation coefficient begins to stabilize when $f_c = 7.3$ Hz. As shown in Figure 8b, the correlation coefficient between A_P and LF/HF was 0.879, indicating a strong correlation. When $f_c = 7.3$ Hz, Figure 8b is obtained from 20 experimental data. In addition, we compared the variability of A_P and LF/HF obtained when the amplitude of the blood pressure pulse wave was at its maximum in 20 experiments. The mean values, standard deviations, and coefficients of variation in the amplitude A_P and the index LF/HF of the blood pressure pulse wave are shown in Table 1. The coefficients of variation for A_P and LF/HF were 0.210 and 0.183, respectively, and we confirmed that the effect of variability was 12.8% lower for LF/HF . Therefore, by using the ratio of the low-frequency component LF to the high-frequency component HF of the blood pressure pulse wave, it is possible to discriminate the wearing condition of the blood pressure pulse wave measurement device with small variation.

Table 1. Comparison of the variability between the amplitude of blood pressure A_P and discriminant index LF/HF .

	Amplitude of Blood Pressure Pulse Wave A_P [mN]	Discriminant Index LF/HF
Average	208	5.74
Standard deviation	43.7	1.05
Coefficient of variation	0.210	0.183

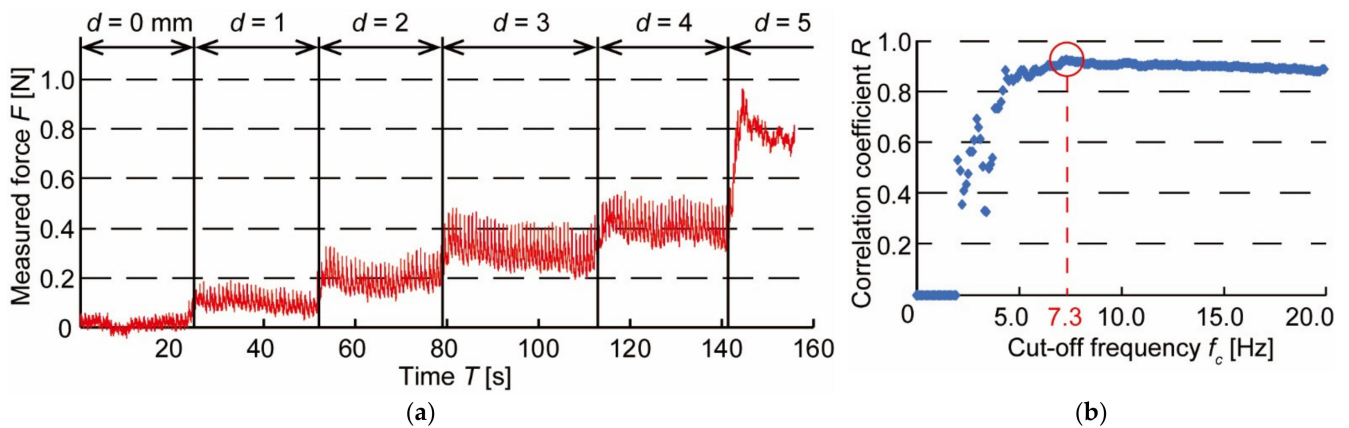


Figure 7. Results of pushing force change experiment: (a) Waveform of blood pressure pulse wave when pushing force is varied; (b) Changes in correlation coefficient between the amplitude of blood pressure A_p and discriminant index LF/HF when cut-off frequency f_c is varied.

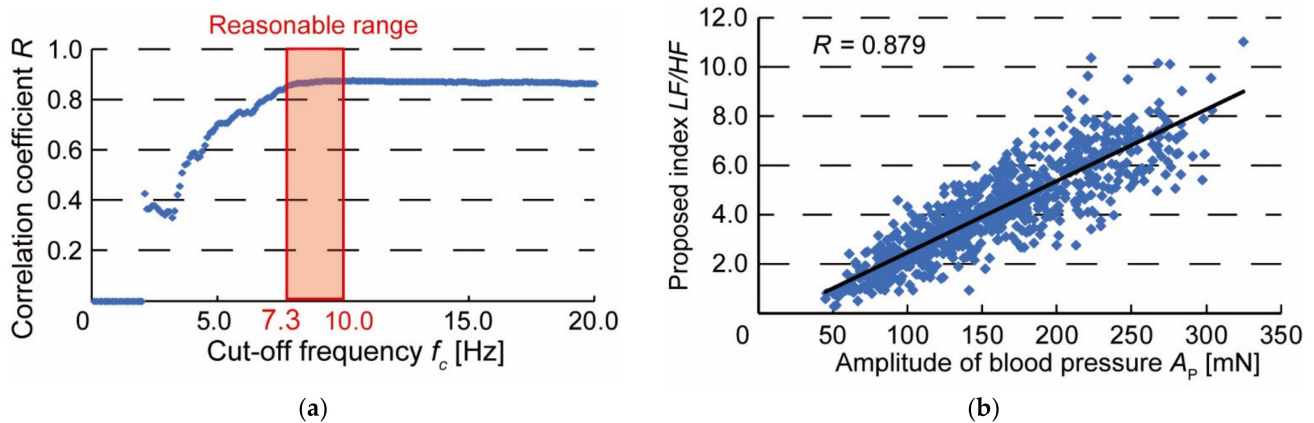


Figure 8. Results of repeated experiments: (a) Changes in correlation coefficient between the amplitude of blood pressure A_p and discriminant index LF/HF when cut-off frequency f_c is varied in repeated experiments; (b) Relationship between amplitude of blood pressure A_p and discriminant index LF/HF when $f_c = 7.3$ Hz.

4. Discussion

In Figure 6c, the blood pressure pulse wave was frequency analyzed by Fourier transform. When $f > 12$ Hz, the spectral intensity of the blood pressure pulse wave almost disappears. This is because the main frequency component of the blood pressure pulse wave is below 12 Hz [18] and the frequency component of the blood pressure pulse wave measured in this experiment is considered to be similar to that reported.

In Figure 7b, the cut-off frequency f_c at which the correlation coefficient between the amplitude of the blood pressure pulse wave, A_p , and the proposed index, LF/HF , reached its maximum was 7.3 Hz. Indicating that the low-frequency component, LF , is the main frequency component of the blood pressure pulse wave. Since f_c is less than 12 Hz, it can be seen that the low-frequency component LF was extracted from the frequency component of the main blood pressure pulse wave. Therefore, LF is the blood pressure pulse wave component with a strong correlation with A_p , while the high-frequency component HF is the blood pressure pulse wave component with little relationship to A_p . In other words, the discriminant index LF/HF indicates the relative magnitude of the pulse wave component with the device wearing condition. Compared with A_p , the low-frequency component LF is thought to accumulate features of the blood pressure pulse wave that are related to the degree of arterial stiffness and atrial contraction, including A_p [19,20]. Observation of these

features is difficult when the device is not approximately worn, and the components are buried in noise. Therefore, there was a strong correlation between A_p and LF/HF , which is the ratio of waveform components and noise related to the wearing state. On the other hand, if the heart rate differs depending on the subject's condition (e.g., after exercise) or individual differences, and if the volume of blood pushed out by the heart per unit time changes, the cut-off frequency f_c is considered to be affected. In such cases, the optimal cut-off frequency in Figure 7b will change.

Figure 8b shows the correlation between the amplitude of the pulse wave, A_p , and the discriminant index, LF/HF when the pressing force experiment was conducted 20 times. Although the optimal cut-off frequency f_c varied from experiment to experiment, the correlation coefficient was calculated by fixing f_c at 7.3 Hz. However, the cut-off frequency must be determined for each subject because it may vary with heart rate and respiration rate. If the heart rate is different from normal, such as during exercise, the heart rate should be calmed down until it reaches a resting state. In addition, the coefficient of variation calculated in Table 1 tends to increase with the value of f_c . Therefore, in this experiment, the effect of variation can be reduced by determining f_c in the range of 7.3–10 Hz, as shown in Figure 8a. It was no longer necessary to confirm that the discriminant index was at its maximum, and the time required to properly attach the device was greatly reduced. We suggest that this is a discriminant index of the wearing condition of a wearable device for easy and accurate blood pressure measurement.

5. Conclusions

In this study, we developed a prototype of a pulse wave measurement device that can be worn in different ways and measured the pulse wave using the arterial tonometry method. The measured waveform was analyzed by frequency and decomposed into high-frequency components HF and low-frequency components LF . We defined LF/HF as a new discriminant index, and the amplitude of the blood pressure pulse wave used to evaluate the wearing condition was compared. When the cut-off frequency was set at 7.3 Hz, the correlation coefficient between the amplitude of the blood pressure pulse wave and the discrimination index was $R = 0.879$. The coefficient of variation was reduced by 12.8% in the discriminant index compared to the amplitude of the blood pressure pulse wave. Therefore, the discriminant index is an index that can evaluate the wearing condition of the blood pressure pulse wave measurement device with a small influence of variation.

Author Contributions: Conceptualization, T.D. and Y.O.; methodology, Y.O.; experiments and analysis, Y.O.; writing—original draft preparation, Y.O.; writing—review and editing, T.D.; supervision, T.D.; All authors have read and agreed to the published version of the manuscript.

Funding: This research received no external funding.

Conflicts of Interest: The authors declare no conflict of interest.

References

1. Psaty, B.M.; Furberg, C.D.; Kuller, L.H.; Cushman, M.; Savage, P.J.; Levine, D.; O'Leary, D.H.; Bryan, R.N.; Anderson, M.; Lumley, T. Association Between Blood Pressure Level and the Risk of Myocardial Infarction, Stroke, and Total Mortality. *Arch. Intern. Med.* **2001**, *161*, 1183–1192. [[CrossRef](#)] [[PubMed](#)]
2. Castillo, J.; Leira, R.; Garcia, M.M.; Serena, J.; Blanco, M. Blood pressure decrease during the acute phase of ischemic stroke is associated with brain injury and poor stroke outcome. *Stroke* **2004**, *35*, 520–527. [[CrossRef](#)] [[PubMed](#)]
3. Lewis, P.S. Oscillometric measurement of blood pressure a simplified explanation. A technical note on behalf of the British and Irish hypertension society. *J. Hum. Hypertens.* **2019**, *33*, 349–351. [[CrossRef](#)] [[PubMed](#)]
4. Noda, A.; Okada, T.; Hayashi, H.; Yasuma, F.; Yokota, M. 24-hour ambulatory blood pressure variability in obstructive sleep apnea syndrome. *Chest* **1993**, *103*, 1343–1347. [[CrossRef](#)] [[PubMed](#)]
5. Mansoor, G.A.; White, W.B. Olecranon bursitis associated with 24-hour ambulatory blood pressure monitoring. *Am. J. Hypertens.* **1994**, *7*, 855–856. [[CrossRef](#)] [[PubMed](#)]
6. Dohi, T.; Waki, K. Blood pressure pulse wave measurement using a wristband type device with 3-axis force sensor. *Int. Symp. Micro-Nano Sci. Technol.* **2016**, *2016*, SuA1-B-8.

7. Dohi, T.; Urata, H.; Fukahori, S.; Hori, M.; Nakai, A.; Nakamura, H. A Continuous and Wearable Blood Pressure Measurement Device with MEMS 3-Axis Force Sensor Array. In Proceedings of the Transducers 2019 International Conference on Solid-State Sensors, Actuators and Microsystems, Berlin, Germany, 23–27 June 2019; pp. 2182–2184.
8. Sato, M.; Dohi, T. Blood pressure pulse wave device with 5-axis adjusting mechanism. *Robomech* **2016**, *2P1-02b5*. (In Japanese) [[CrossRef](#)]
9. Dueck, R.; Goedje, O.; Clopton, P. Noninvasive continuous beat-to-beat radial artery pressure via TL-200 applanation tonometry. *J. Clin. Monit. Comput.* **2012**, *26*, 75–83. [[CrossRef](#)] [[PubMed](#)]
10. Kato, Y.; Hamaguchi, T. Sensor technology to realize continuous blood pressure monitoring. *Omron Tech.* **2018**, *50*, 26–34.
11. Canning, J.; Helbert, K.; Iashin, G.; Matthews, J.; Yang, J.; Delano, M.K.; Sodini, C.G.; Zhang, Q. Noninvasive and continuous blood pressure measurement via superficial temporal artery tonometry. In Proceedings of the 2016 38th Annual International Conference of the IEEE Engineering in Medicine and Biology Society, Orlando, FL, USA, 16–20 August 2016; pp. 3382–3385.
12. Shimura, K.; Hori, M.; Dohi, T.; Takao, H. The Calibration Method for Blood Pressure Pulse Wave Measurement Based on Arterial Tonometry Method. In Proceedings of the 2018 40th Annual International Conference of the IEEE Engineering in Medicine and Biology Society, Honolulu, HI, USA, 18–21 July 2018; pp. 3642–3645.
13. Osawa, Y.; Hata, S.; Hori, M.; Dohi, T. Comparison of Features by Simultaneous Measurement of Blood Pressure Pulse Wave and Electrocardiogram. In Proceedings of the 2020 42nd Annual International Conference of the IEEE Engineering in Medicine and Biology Society, Montreal, QC, Canada, 20–24 July 2020; pp. 4664–4667.
14. Osawa, Y.; Hata, S.; Hori, M.; Dohi, T. Analysis of Blood Pressure Pulse Wave and Electrocardiogram Waveforms Measured by a Wearable Device with MEMS Sensors. *Sens. Mater.* **2021**, *33*, 1063–1072. [[CrossRef](#)]
15. Kemmotsu, O.; Ueda, M.; Otuka, H.; Yamamura, T.; Okamura, A.; Ishikawa, T.; Winter, D.C.; Eckerle, J.S. Blood pressure measurement by arterial tonometry in controlled hypotension. *Anesth. Analg.* **1991**, *73*, 54–58. [[CrossRef](#)] [[PubMed](#)]
16. Takahashi, H.; Nakai, A.; Thanh-Vinh, N.; Matsumoto, K.; Shimoyama, I. A triaxial tactile sensor without crosstalk using pairs of piezoresistive beams with sidewall doping. *Sens. Actuators* **2013**, *199*, 43–48. [[CrossRef](#)]
17. McKenzie, I. Heart rate and blood pressure variability in subjects exposed to simulated increases in gravity. *Exp. Physiol.* **1993**, *78*, 825–834. [[CrossRef](#)] [[PubMed](#)]
18. Holdsworth, D.W.; Norley, C.J.D.; Frayne, R.; Steinman, D.A.; Rutt, B.K. Characterization of common carotid artery blood-flow waveforms in normal human subjects. *Physiol. Meas.* **1999**, *20*, 219–240. [[CrossRef](#)] [[PubMed](#)]
19. Safar, M.E.; Asmar, R.; Benetos, A.; Blacher, J.; Boutouyrie, P.; Lacolley, P.; Laurent, S.; London, G.; Panni, B.; Protogerou, A. Interaction between hypertension and arterial stiffness an expert reappraisal. *Hypertension* **2018**, *72*, 796–805. [[CrossRef](#)] [[PubMed](#)]
20. Masuda, Y.; Hirai, A.; Ozawa, S.; Fukushima, K. The prejection waves in the arterial pulse waves. *Cardiovasc. Sound Bull.* **1974**, *4*, 273–280. (In Japanese)